IIETA International Information and Engineering Technology Association
Advancing the World of Information and Engineering

Mathematical Modelling of Engineering Problems
Vol. 9, No. 4, August, 2022, pp. 1113-1122
Journal homepage: http://iieta.org/journals/mmep

Real-Time Implementation of an Enhanced PID Controller Based on Ant Lion Optimizer for Micro-Robotics System

Ehab S. Ghith*, Farid A. Tolba

Department of Mechatronics, Faculty of Engineering, Ain Shams University, Cairo 11566, Egypt

Corresponding Author Email: Drehabghith1978@gmail.com

https://doi.org/10.18280/mmep.090430

Received: 6 June 2022
Accepted: 2 August 2022

Keywords:
PID controller, micro-particles robotics, grey wolf optimization (GWO), harmony search algorithm (HS), ant lion optimizer (ALO), minimally invasive surgery(MIS)

ABSTRACT

Microparticles have the potentials to be used for many medical purposes in-side the human body such as drug delivery and other operations. This paper offers a comprehensive comparative study of three meta-heuristic search algorithms for controlling the micro-robotics system with a proportional-integral-derivative (PID) controller. Grey Wolf Optimization (GWO), Harmony Search algorithm (HS) and Ant Lion Optimizer (ALO) are the various techniques that this study adopts. The optimum position control can be obtained by employing the former algorithms with different fitness functions, namely Integral Absolute Error (IAE), Integral of Time Multiplied by Square Error (ITSE), Integral Square Time multiplied square Error (ISTES), Integral Square Error (ISE), Integral of Square Time multiplied by square Error ((ISTSE), and Integral of Time multiplied by Absolute Error (ITAE). In a MATLAB Simulink, each control method was presented, while the experimental measurements were tested and operated by the LabVIEW Software. It is observed that the HS technique achieves the highest values of settling error for both simulation and experimental results among other control approaches, while the ALO approach reduces the settling error by 32.5% compared to former experiments. The results indicate that ALO is the best method among all approaches and that ISTES is the best choice of PID for optimizing the controlling parameters.

1. INTRODUCTION

For minimizing the trauma of surgical patients, minimal invasive surgery (MIS) is recommended than orthodox open heart syrgery because it provides clinicians the comfort to go deep in every site of the human body. Along with that, thanks to the minimal invasive surgery, patients are required to spend less time in hospitals [1]. Hence, it is also a cost-effective option. Laparoscopy is one of such surgeries which are implemented these days. Theinstruments used in this process are usually small, and the operation is conducted by observing the images taken through the instrumental camera. Different variances of the two surgical methods are exhibited in Figure 1.

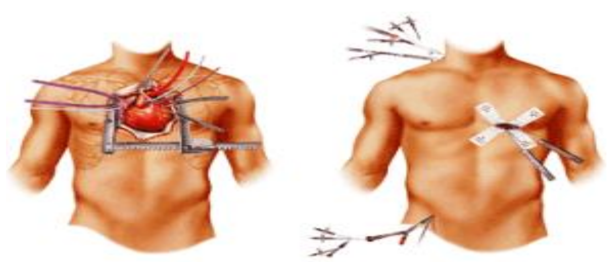

Figure 1. The image on the left depicts an orthodox open heart surgery, while the image on the right indicates laproscopy as a mininally invasive heart surgery [1]

MIS can be also advantageous in medicine when it is robot-used, thanks to its minimization invasiveness. Moreover, the treatment of previously inoperable patients is facilitated by this method. As an implementation of such robotic system, the needles are accurately guided to the specified site in the human body. They are associated with the organs in the human body via veins, arteries and the gastrointestinal tract, and they are utilized to target the organ as specifically required for diagnosis, treatment and drug delivery. The smaller the robot is, the better because the penetration depth can be increased inside the human body. This will also lead to medicine efficiently travelling in smaller pathways for the achievement of such goal.

Keuning et al. [2] offered effectively constructed paramagnetic micro-particles for the spherical site, with 8.4 µm settling error, as the system arrives to the control position. These micro-particles were of an average diameter of 100 µm, with a hollow coil used in the experiment and the working media was water. Farag et al. repeated the same experiment [3], but with a solid coil and a settling error of 8 µm. The current study repeats the same experiment, but with a settling error of 5.4 µm. The ALO approach was observed to reduce the error rate up to 32.5% in comparison with the previous experiments.

In order to achieve control goals, a sufficient and suitable design of controller is necessary. Although different control methods have been developed, PID is still used because of being tunable, its easy implementation, and the quite simple structure of PID [4-10]. However, a difficulty still lies in properly tuning the PID controller to the extent of becoming optimally efficient. Different designs were proposed, and among them was PID control best-known methods: Ziegler and Nichols, but it is not easy to reach the greatest performance of this method [11, 12]. Moreover, extra complex mathematical calculations are required for the usual method tuning. Nevertheless, this can be avoided by proposing different tuning methods and artificial intelligence-based optimization methods.

Meta-heuristic algorithms are supported by the use of multiple optimization techniques in different engineering fields. No gradient information is required for these techniques, and they are flexible and easily implementable comparatively. Single-based or population-based algorithms are included under meta-heuristic techniques. In single-based or trajectory optimization algorithms, a single optimal solution is generated. However, in other algorithms, such as population-based, multiple solutions which are often redundant in nature can be generated. Optimization algorithms can include five major types: Human, chemical, swarm intelligence, physics, and evolutionary-based optimization algorithm [13-41].

Our contribution in the present study is clear in the following two points:

(1) All the previous research in the literature review is found to focus on only the ITAE fitness function. However, our present study offers comparative analyses of six different fitness functions, namely ISTSE, ITSE, ISE, ISTES, ITAE, and IAE through processing to reach the best one among them that can achieve the PID controller optimum parameters, such as K_p, K_i, and K_d. The study adopts better fitness functions for comparing the dynamic characteristics of different control techniques, in terms of settling and rising time which are not investigated thoroughly in the previous studies.

(2) The three meta-heuristic search algorithms, GWO, HS, and ALO will be addressed and compared experimentally and numerically according to the best fitness function obtained for tuning the PID controller, with respect to their settling, rising time, and settling errors. This was not offered an in-depth investigation in the previous studies.

The current study also includes mathematical model of micro-robotics system, PID controller, fitness function types, optimization techniques, and the description system architecture in part 2. In part 3, the simulation, experimental results, and discussion are depicted, while part 4 exhibits the future prospects and conclusion of this study. The data is collected by an experimental setup, of which some results are reported by Farag et al. [3] which is an extension of this work.

2. RESEARCH METHOD

2.1 Mathematical model

Paramagnetic material is employed for the design of particles formed by iron-oxide in lactic acid. With 100μm diameter, the velocity of these particles is dependent on two factors. Depending on the coils magnetic field, the micro-particles induce the magnetic forces and viscous drag. Furthermore, if acceleration reaches zero, maximum velocity is achieved, and magnetic and viscous drag forces become equal. The magnetic force can be defined by the following equation.

$$F = \nabla \alpha_p V_p B^2 \tag{1}$$

where, V_p denotes the particles volume, while B denotes magnetic flux density. Magnetic flux density is time- and distance-dependent, while V_p and α_p are the constants. The variables given below are used for the substitution of V_p for force production, as indicated by the equation given below.

$$F = \frac{4}{3}\pi \alpha_p r_p^3 \nabla B^2 \tag{2}$$

where, r_p denotes the micro-particles radius, while the following equation is employed for drag force.

$$F_d = -6\pi\eta r_p v \tag{3}$$

where, r_p denotes the micro-particles radius, while the following equation is employed for drag force.

$$\begin{gathered} \sum F = m_p a_p \\ \tfrac{4}{3}\pi \alpha_p r_p^3 \nabla^2 - 6\pi\eta r_p v = m_p a_p \\ v = \frac{\frac{4}{3}\pi \alpha_p r_p^3 \nabla B^2 - m_p a_p}{6\pi\eta r_p} \end{gathered} \tag{4}$$

When particles' acceleration is equal to zero, maximum velocity is achieved by micro-particles in Eq. (4). A calculation of the maximum velocity is conducted by the following equation:

$$v_m = \frac{2}{9}\frac{\alpha_p r_p^2}{\eta} \nabla B^2 \tag{5}$$

Particles with spherical shape were considered perfect, while F_m is employed for denoting the stimulated utilizing force. With respect to liquid, the particles' speed was associated with the drag force that F_d represents. In case of stable liquid, the particle's speed is associated with the drag. A continuous time model can be designated by the following equation:

$$m\ddot{x} + C_d * \dot{x} = F_m \tag{6}$$

As observed by C_d, drag *via* drag Stokes of Reynolds is continuously designated as low, the acceleration is represented by $\ddot{x}$, velocity is represented by $\dot{x}$, while m denotes particle's mass. The following formula represents the micro-particle's transfer role:

$$\frac{X(s)}{F_m(s)} = \frac{1}{ms^2 + C_d * s} \tag{7}$$

2.2 PID controller

One of the major controller types applicable in industrial use is Ideal-PID. It can improve the steady-state and transient errors. However, the ideal-PID high performance is lost upon occurrence of disturbances. The same algorithm (or with variations to it) is usually employed by feedback control loops [42]. These gains are proportional gain K_p, integral gain K_i, and derivative gain K_d. Each gain can act on the error usually achieved by the subtraction of a measured variable, i.e., the output from set point inserted by the user. The PID controller's transfer function is exhibited in Eq. (8). Figure 2 illustrates the PID controller standard form, while Figure 3 presents the tuning PID controller's basic structure.

$$C_{PID}(s) = \frac{Y(s)}{E(s)} = K_p + \frac{K_i}{s} + K_d s \quad (8)$$

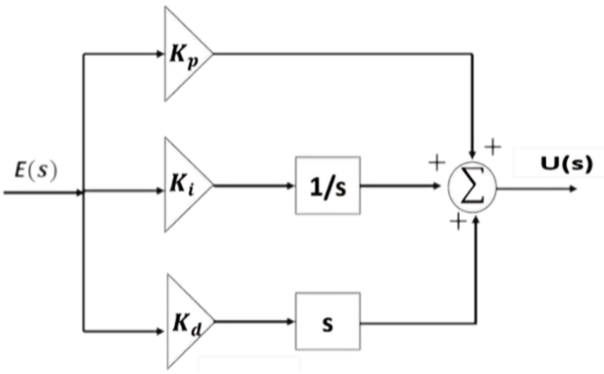

Figure 2. Ideal PID controller

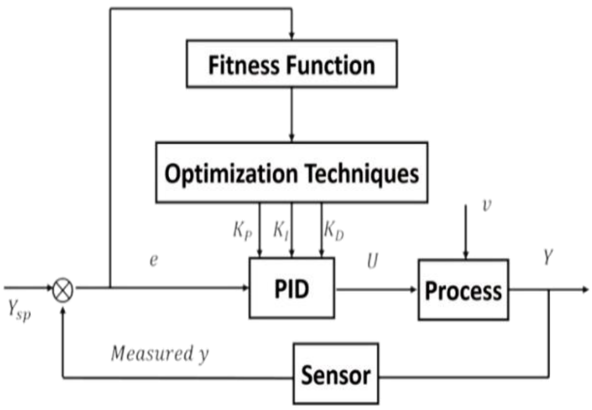

Figure 3. Block diagram of tuning PID controller

The five main components of tuning PID controller are the fitness function, optimization techniques, PID, process, and the sensor. The first component which is the fitness function type such as Integral Absolute Error (IAE), Integral Square Error (ISE), Integral of Time multiplied Absolute Error (ITAE), Integral of Time multiplied square Error (ITSE), Integral Square Time multiplied square Error (ISTES), or Integral of Square Time multiplied by square Error (ISTSE). The second component is the optimization techniques such as Grey Wolf Optimization (GWO), Harmony Search Algorithm (HS) or Ant Lion Optimization (ALO). The third component is the PID consists of three parameters which are K_p, K_i, and K_d. The fourth component is the process and it is based on micro robotic system. Finally, the last component is the sensor such as camera.

2.3 Fitness functions types

The design of any controller type requires different optimum control parameters. Distinct parameters are calculated in order to reduce the objective function. Time-dependency is an error that demands multiple functional objectives. The different fitness function types are defined by the equations below [43-45]:

Integral Absolute Error (IAE):

$$IAE = \int_0^\infty |e(t)|dt \quad (9)$$

Integral Square Error (ISE):

$$ISE = \int_0^\infty e^2(t)\, dt \quad (10)$$

Integral of Time multiplied Absolute Error (ITAE):

$$ITAE = \int_0^\infty t|e(t)|dt \quad (11)$$

Integral of Time multiplied square Error (ITSE):

$$ITSE = \int_0^\infty te^2(t)dt \quad (12)$$

Integral Square Time multiplied square Error (ISTES):

$$ISTES = \int_0^\infty [t^2 e(t)]^2 dt \quad (13)$$

Integral of Square Time multiplied by square Error (ISTSE):

$$ISTSE = \int_0^\infty t^2 e^2(t)dt \quad (14)$$

The following rules formulate the optimization problem, i.e., objective function is minimized and subjected to:

$$K_{pmin} < K_p < K_{pmax}$$
$$K_{imin} < K_i < K_{imax}$$
$$K_{dmin} < K_d < K_{dmax}$$

2.4 Optimization techniques

The methodologies of optimization used in this study include Grey Wolf Optimization (GWO), Harmony Search Algorithm (HS) and Ant Lion Optimizer (ALO).

2.4.1 Grey Wolf Optimization (GWO)

Grey Wolf Optimization (GWO) algorithm is an up-to-date technique that Mirjalili et al. introduced in 2014 [46]. Four main types of simulations appear in the grey wolves' hierarchy. In these types, Alpha (α) is the leader that offers the best solution, the second-best solution is Beta(β) that plays a role to assist alpha in any decision process, the third-best solution is Delta(δ), and the remaining Omega(ω) population is deemed the worst-ranked. A description of the flowchart is given below in Figure 4. Below are the mathematical equations of GWO:

$$\vec{D} = |\ \vec{C}.\overrightarrow{X_p(t)} - \overrightarrow{X(t)}| \quad (15)$$

$$\overrightarrow{X(t+1)} = \overrightarrow{X_p(t)} - \vec{A}.\vec{D} \quad (16)$$

It is clear from this equation that t refers to the current iteration, while $\vec{A}$ and $\vec{C}$ depict the vector of coefficients. $X_p(t)$

points to the vector position reached up to this point in optimal solution, and $\overrightarrow{X}$ is GWO position vector. A calculation of $\vec{A}$ and $\vec{C}$ can be given by the following equation:

$$\vec{C}=2.\vec{r} \tag{17}$$

$$\vec{A}=2\,\vec{a}.\vec{r}-\vec{a} \tag{18}$$

This equation shows that $\vec{a}$ stands for the variable decreasing linearly from 2 to 0 during a series of iterations. In this equation, r depicts the vector present randomly in the interval ranging from 0 to 1. The top three best solutions are then saved and searched on different search agents by the algorithm, with omegas included. Their position is updated by using the position of the best search agents. A definition of beta, alpha, omega, and delta is provided in the equation below:

$$\overrightarrow{D_\alpha}=|\overrightarrow{C_1}.\overrightarrow{X_\alpha}-.\overrightarrow{X}|,\ \overrightarrow{D_\beta}=|\overrightarrow{C_2}.\overrightarrow{X_\beta}-.\overrightarrow{X}|,\ \overrightarrow{D_\delta}=|\overrightarrow{C_3}.\overrightarrow{X_\delta}-.\overrightarrow{X}| \tag{19}$$

$$\overrightarrow{X_1}=\overrightarrow{X_\alpha}-\overrightarrow{A_1}.(\overrightarrow{D_\alpha}),\ \overrightarrow{X_2}=\overrightarrow{X_\beta}-\overrightarrow{A_2}.(\overrightarrow{D_\beta}),\ \overrightarrow{X_3}=\overrightarrow{X_\delta}-\overrightarrow{A_3}.(\overrightarrow{D_\delta}) \tag{20}$$

$$\overrightarrow{X(t+1)}=\frac{\overrightarrow{X_1}+\overrightarrow{X_2}+\overrightarrow{X_3}}{3} \tag{21}$$

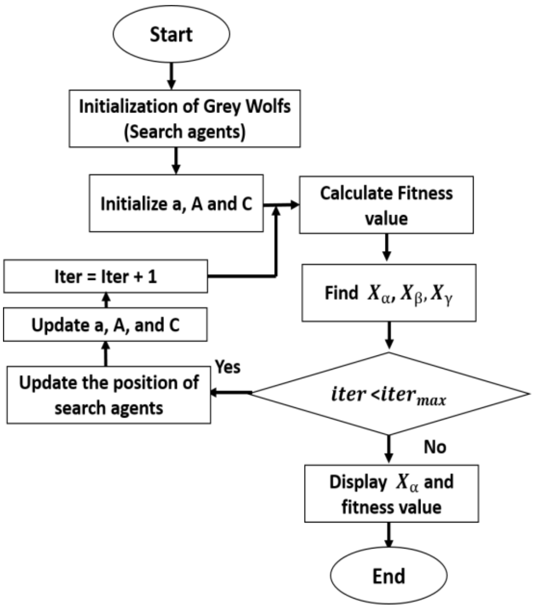

Figure 4. Flowchart of the GWO Algorithm [46]

2.4.2 Harmony Search Algorithm (HS)

This algorithm was developed in 2001 by Geem and is based on the musicians' concept of polishing the pitches for achieving the best state of harmony. Figure 5 exhibits the flow chart of this algorithm of optimization [47].

The steps of HAS are given below.

• Initialize

• X_i defines the design variables and is in the range of (i=1, 2, ….., N), where N represents the number of design variables.

• The upper and lower boundary for each variable design in which $X_i^L \le X_i \le X_i^U$ must be defined.

$$X_i^j = X_i^L + (X_i^U - X_i^L) * rand(1,N) \tag{22}$$

• The harmony memory size (HMS) is the number of population and defined by X_i^j in which j represents 1, 2…. HMS.

• The maximum iteration number is set.

• The harmony memory consideration rates (HMCR) need to be adjusted within a range of 0 ≤HMCR≤ 1 out of which 0.95 is the most suitable value of HMCR.

• The step size can be computed by $b_i = \frac{X_i^U - X_i^L}{N}$ and 0.2 is the most common value of b_i.

• Pitch adjustment rate i.e. PAR should be adjusted depending upon a specific range from $0 \le PAR \le 1$ and 0.3 is the most common value of PAR.

• The objective functions (F), and the harmony memory (HM) in the matrix is defined by the following equations.

$$HM = \begin{bmatrix} X_1^1 & X_2^1 & X_N^1 \\ X_1^2 & X_2^2 & X_N^2 \\ X_1^{HMS} & X_2^{HMS} & X_N^{HMS} \end{bmatrix} \tag{23}$$

$$F = \begin{bmatrix} F(X^1) \\ F(X^2) \\ \cdots \\ F(X^{HMS}) \end{bmatrix} \tag{24}$$

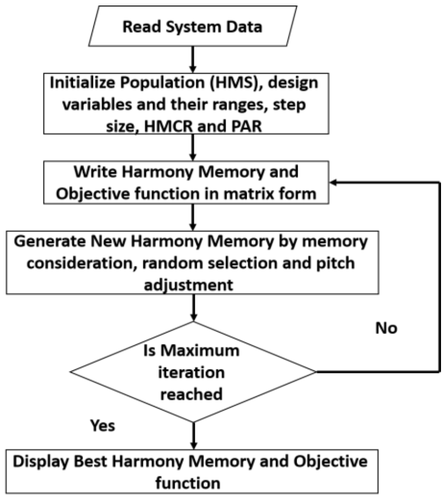

Figure 5. HS algorithm's flow chart [47]

• Next step is improvisation in which each iteration generates a new harmony according to the following criteria

• Two main values are produced by the pitch adjustment operation and if the found probability is (1- PAR), any kind of amount is not added but in case of use of PAR, an added new harmony would be calculated by:

$$X_i' = X_i' \pm b_i \tag{25}$$

• The new harmony is selected in a random way in which $X' = (X_1', X_2', \dots X_N')$ and it uses the probability of (1- HMCR).

• The HMCR probability is used to determine the consideration of memory which is based upon X_i' for $(X_1', X_2', \dots X_i^{HMS})$.

• Lastly, the fitness function (F) and HM value update is minimized in order to eliminate the harmonies with the worst values. This update is repeated till the maximum number of iterations or optimum solution is achieved.

2.4.3 Ant Lion Optimizer (ALO)

Another metaheuristic algorithm is the ant lion algorithm or ALO, and is considered as the nature based type which is capable of dealing with uni and multidimensional problems and was described by Mirjalili et al in 2015. This algorithm depends upon the hunting nature of grey antlions in which exploration and exploitation is achieved by global and local search. Furthermore, ALO also explores multiple other regions for the improvement of exploration phase. The process of hunting by antlions is divided into 5 stages walk of ants, traps building, falling of ants into the traps, movement of ants towards antlion, catching and rebuilding the traps [48].

Stage 1: Walk of ants

Antlion and ant must have a great interaction between each other so, when the prey moves to search food and shelter, antlion starts putting traps to be able to hunt the prey. The movement of prey is stochastic and does a random walk. Following equation describes the movement's random modelling.

$$X(t) = [0, cusum(2r(t_1), \dots\dots\dots cusum(2r(t_n - 1)] \tag{26}$$

here, the accumulated sum is designated as *cusum*, the steps of the random walk are denoted by *t*, random movement function is denoted by $r(t_1)$ and maximum iteration is given by $r(t_1)$. This function is proved by given equation.

$$r(t) = \begin{cases} 1\ if\ rand > 0.5 \\ 0\ if\ rand \leq 0.5 \end{cases} \tag{27}$$

here, generated random values which are within the range [0, 1] is denoted by rand whereas following equation suggests normalizing ant's random walk,

$$X_i(t) = \frac{(x_i^t - a_i) * (d_i^t - c_i^t)}{(b_i - a_i)} + C_i^t \tag{28}$$

In this equation lower and upper walking number are given by a_i and b_i associated with i[th] variable whereas lower and upper variables at t[th] iteration are designated as C_i^t and d_i^t respectively.

Stage 2: Building trap

Here the fittest antlion is searched by applying the roulette wheel by ALO and thus it has the highest probability of catching the prey.

Stage 3: Entrapments of ants in traps

The relationship between the walk of ants the traps direction set by antlions can be calculated by following equation.

$$C_i^t = Antlion_j^t + C^t \tag{29}$$

$$d_i^t = Antlion_j^t + d^t \tag{30}$$

here, the random walk's hypersphere is denoted by vector *C* and *d* whereas lower and upper values are denoted by C^t and d^t which resulted at t[th] iteration.

Stage 4: Moving of the prey towards the antlion

If ants fall into the trap and antlion realizes that, it throws sand in the direction of pit's edge. This behavior is explained by using following equation.

$$C^t = \frac{C^t}{I} \tag{31}$$

$$d^t = \frac{d^t}{I} \tag{32}$$

here, total number of iteration are given by *T*, *W* represents a constant value and *I* is the ratio based on total iterations number. This ratio is evaluated by following:

$$I = 10^w \frac{t}{T} \tag{33}$$

Stage 5: Catch prey and re-build traps

The ants when caught by the antlions in the trap, this stage is considered as the last hunting stage. If the capture ant is fitter than antlion, it suggests that the ant is captured by the antlion. Antlion after trapping updates its current position and build a new trap for catching a new prey. This step is simulated by following equation.

$$Antlion_j^t = Ant_i^t\ if\ f\left(Ant_j^t\right) > f(Antlion_j^t) \tag{34}$$

here, ant and antlion's fitness function is denoted by f(), *t* gives the current iteration number and location of j[th] antlion at t[th] iteration is represented by $Antlion_j^t$.

Stage 6: Elitism

In this step, optimal solution is collected on the basis of previous ALO stages. Here having the eite antlions obtained during each iteration is the best solution. The random movement of ants towards antlion and elite one is given by following equation.

$$Ant_i^t = \frac{R_A^t + R_E^t}{2} \tag{35}$$

In this equation the random walk towards antlion at t[th] iteration is represented by R_A^t, Ant_i^t is i[th] prey located at t[th] iteration, and R_E^t is the random walk performed in the elite antlion's direction.

Designing the tuning parameters of PID depending upon ALO:

This algorithm is applied to identify the control parameters which are optimum and include K_P, K_I, and K_D. The steps required to search the optimal parameters include:

(1) Defining variables such as population of antlions, ants and the total iterations. These are set by boundaries for PID parameters which are given as maximum and minimum values.

(2) For holding the ants' position, a matrix is designed. This matrix has n and d dimension in which d indicates PID parameters, and n is the prey numbers. This description is given in the form of the matrix given below.

$$M_{ant} = \begin{bmatrix} A_{11} & A_{12} & \dots & A_{1d} \\ A_{21} & A_{22} & \dots & A_{2d} \\ : & : & : & ; \\ A_{n1} & A_{n2} & \dots & A_{nd} \end{bmatrix} \tag{36}$$

(3) Afterwards, the evaluation of prey's position is based upon the function of fitness. This fitness function is described by the fitness matrix called as M_{FA}. Here *f* indicates objective function or fitness.

$$M_{FA} = \begin{bmatrix} f(A_{11} & A_{12} & \dots & A_{1d}) \\ f(A_{21} & A_{22} & \dots & A_{2d}) \\ : & : & : & ; \\ f(A_{n1} & A_{n2} & \dots & A_{nd}) \end{bmatrix} \tag{37}$$

(4) The antlions hide somewhere in the search space, and fitness value and position are sorted in the matrix such as M_{FAL} and $M_{antlion}$, in which antlions number is given as n.

$$M_{FAL} = \begin{bmatrix} f(AL_{11} & AL_{12} & \dots & AL_{1d}) \\ f(AL_{21} & AL_{22} & \dots & AL_{2d}) \\ \vdots & \vdots & \vdots & ; \\ f(AL_{n1} & AL_{n2} & \dots & AL_{nd}) \end{bmatrix} \quad (38)$$

$$M_{antlion} = \begin{bmatrix} AL_{11} & AL_{12} & \dots & AL_{1d} \\ AL_{21} & AL_{22} & \dots & AL_{2d} \\ \vdots & \vdots & \vdots & ; \\ AL_{n1} & AL_{n2} & \dots & AL_{nd} \end{bmatrix} \quad (39)$$

(5) Considerin M_{FAL} matrix, the best fitness function is initially selected and depending upon that corresponding antlion is selected which is also known as the most optimum antlion.

(6) Specific antlion is selected through the roulette wheel, and position is updated by using the equations in which current iteration and position are directly proportional to each other.

(7) Lastly, ants conduct a random walk and normalized in the search space direction of each prey according to the equation given above. After that the ants' position is updated according to the equation given above.

(8) The fitness values of ant is evaluated and the value of antlion along with its prey is substituted if they have a better fitness value.

(9) The position of antlion is updated if it shows the best value of fitness, this happens when antlion exhibits a better fitness value than a current one.

(10) All the steps are repeated till the maximum iteration number is achieved, and at the end a best parameter is selected.

2.5 System architecture

A total of eight components makes up this system, including micro-particles, control algorithm, pantograph robot, reservoir, real-time controller, coils, camera, microscope, and a power supply unit. Figure 6 denotes these main 2D space components.

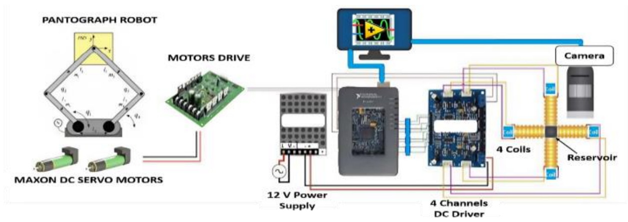

Figure 6. Micro-particle's complete system architecture in 2D space [3]

3. RESULTS AND DISCUSSIONS

3.1 Simulation and experimental results

This section offers comprehensive details for investigating the performance of the micro-robotic system by using various advanced control methods. Different tests are employed for executing and assessing the performance of various control techniques. An evaluation of different approaches is conducted at a particular position for standardization. For instance, 1,000 μm is used for command reference. Figure 7 presents the Simulink diagram exhibiting different techniques of the micro-robotic system. The proposed system parameters are exhibited in Table 1, and a summary of the input parameters of various techniques is given in Table 2, for the micro-robotic system position to be maintained and controlled at 1,000 μm. The output results of various optimization techniques, regarding time response with different objective functions are presented in Table 3. Table 4 provides a description of the output results of various optimization techniques regarding time response (Practical), on the basis of the best objective function (ISTES). In figure 8, the behavior is represented by tracking the position reference with different fitness functions for best optimization techniques (ALO). Finally, Figure 9 offers a representation of the behavior by tracking the position reference with best fitness function (ISTES) simulation and time response (practical) for best optimization techniques (ALO) and best fitness function (ISTES).

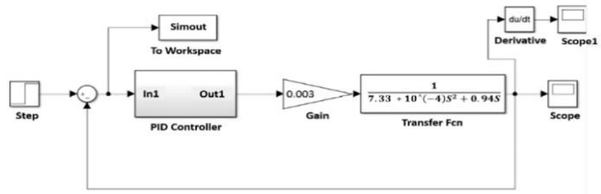

Figure 7. Simulink diagram of the micro-robotic system with different advanced control techniques

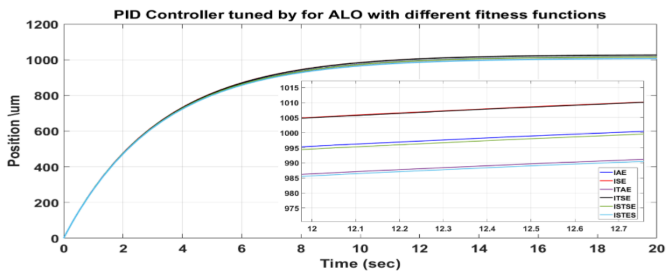

Figure 8. Position behaviour of ALO based on PID control with different fitness functions

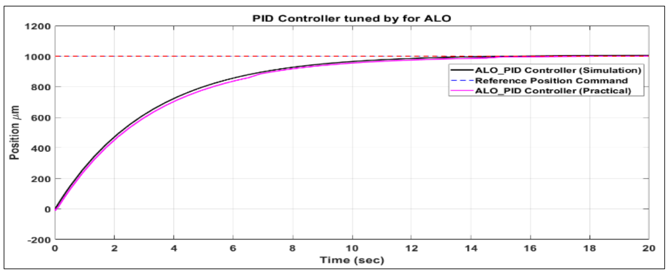

Figure 9. Position behaviour with ALO based PID control

3.2 Discussion

The three optimization strategies are extensively evaluated in this section based on various fitness functions. The parameters consist of settling error, rising time, and settling time-based on the best fitness function (ISTES). Table 4 exhibits the results of the measurements of GWO, HS, and ALO, which were obtained earlier. It was observed that the HS technique achieves the highest values of the rise time, settling time and settling error for both simulation and experimental results among other control approaches. Besides, the amount of settling error is increase by 12.5% compared with the value reported in Ref. [3]. On the other hand, the ALO technique is the best Algorithm compared to other techniques, as it reduces the settling error by 32.5% compared with data published in Ref. [3]. By adopting the GWO technique the settling error is reduced by 0% than other experiments. It can be concluded that the ALO technique is a promising approach for predicting real-time for the micro-robotics system when adopted with the ISTES fitness function, which achieves the best dynamic characteristics.

Table 1. The proposed system parameters

Name	Values	Units
Radius (r)	50	μm
Water density (ρ)	998.2	$Kg.m^{-3}$
Dynamic Viscosity (ζ)	1	mPa s
Mass (m)	$7.33*10^{-10}$	Kg
Drag Coefficient (cd)	$0.94*10^{-6}$	$N.S.m^{-1}$

Table 2. Optimization techniques input parameters

Optimization Techniques	Parameters	Values
All	Number of variables (nVar)	3
	Minimum value of variables (Kmin)	[0 0 0]
	Maximum value of variables (Kmax)	[100 1 1]
	Max number of iterations	25
	Number of Search Agents	30
HS	Harmony Memory Size (HMS)	30
	Harmony Memory Considering Rate (HMCR)	0.95
	Pitch Adjustment Rate (PAR)	0.03
	bw	0.2

Table 3. The output result of various optimization techniques in terms of time response with different objective functions (simulation)

Techniques	(Ideal-PID)	Control parameter			Time response	
		KP	KI	KD	tr	ts
GWO	IAE	100	0.6672	0.0891	6.9391	12.0955
	ISE	100	1	0	6.9574	12.0471
	ISTES	100	1	0	6.9574	12.0471
	ISTSE	100	0.6021	0.0019	6.9310	12.0949
	ITAE	100	0.2929	0	6.8934	12.0781
	ITSE	100	0.2926	0.018	6.8938	12.0788
ALO	IAE	100	0.55445	0	6.9262	12.0955
	ISE	100	1	0	6.9574	12.0471
	ISTES	100	0.2711	0	6.9574	12.0471
	ISTSE	100	0.6051	0	6.9312	12.0948
	ITAE	100	0.2666	0	6.8895	12.0743
	ITSE	100	1	0	6.9574	12.0471
HS	IAE	98.551	0.6363	0.6916	7.0533	12.2806
	ISE	99.069	0.0452	0.9761	6.9355	12.1614
	ISTES	95.974	0.3404	0.5853	7.277	12.6534
	ISTSE	98.004	0.5645	0.7766	7.3537	12.6643
	ITAE	95.073	0.4621	0.4842	7.086	12.3419
	ITSE	94.515	0.9704	0.2007	7.1953	12.5443

Table 4. Time responses comparison among various optimization approaches (Practical) based on best fitness function (ISTES)

No.	Control Technique	t_r	t_s	Settling Error (μm)	Reduced Based on ref. [3]
1	GWO	7.7083	13.1007	8	0%
2	ALO	6.9991	12.8723	5.4	32.5%
3	HS	7.2103	13.2088	9	-12.5%

4. CONCLUSIONS

We established an experimental and numerical investigation to control the position of the micro-robotics system with a PID controller. The numerical investigation and prediction focus on three optimization strategies for tuning the PID controller. All approaches are solved in MATLAB Simulink, and the experimental study is carried out on an experimental setup, with practical results obtained by measurements. Six different fitness functions are employed to predict and identify the best one that achieve the minimum settling error. The main conclusions are summarized as follows:

(1) The ALO achieves the highest performance techniques compared to different algorithms as it enhances the parameter

efficiency of systems by decreasing the error rate up to 32.5%, as compared to former experiments. Hence, the SSA technique is recommended for the tuning of PID parameters.

(2) The ISTES is the best fitness function, as it reduces the settling error other than the various fitness function adopted.

The present investigation indicates some areas where further research is required to apply various optimization techniques for tuning the PID controller for micro-robotics applications, such as sine cosine algorithm (SCA) and hybrid PSO and compare their results with the applicable techniques. Using the current study as a guide, it is proposed that an expansion of the experiments be planned to address the following points:

(1) Conduct further experimental investigations on the large-scale robotics system fitted with comprehensive measuring techniques to discover and gain unprecedented knowledge about its actual dynamic behavior.

(2) Subsequent studies should concentrate on the economic analysis on the micro-robotics systems and their certain applications.

ACKNOWLEDGMENT

I would like to thanks Dr. Mohamed Sallam for his support in the experimental setup.

REFERENCES

[1] Keuning, J. (2011). Image-based magnetic control of Microparticles. Master's thesis, University of Twente. https://purl.utwente.nl/essays/70474.

[2] Keuning, J.D., de Vriesy, J., Abelmanny, L., Misra, S. (2011). Image-based magnetic control of paramagnetic microparticles in water. In 2011 IEEE/RSJ International Conference on Intelligent Robots and Systems, San Francisco, CA, USA, pp. 421-426. https://doi.org/10.1109/IROS.2011.6095011

[3] Farag, R., Badawy, I., Magdy, F., Mahmoud, Z., Sallam, M. (2020). Real-time trajectory control of potential drug carrier using pantograph "Experimental study". In International Conference on Advanced Intelligent Systems and Informatics, pp. 305-313. https://doi.org/10.1007/978-3-030-58669-0_28

[4] Astrom, K.J., Hagglund, T. (1995). PID controllers: Theory, design, and tuning. 2nd ed.: NC: Instrument Society of America.

[5] Mansour, T. (2011). PID controller implementation and tuning. Published by InTech.2011. https://doi.org/10.5772/652

[6] Ogata, K. (2010). Modern control engineering. Prentice-Hall.

[7] Hägglund, T., Åström, K.J. (2002). Revisiting the Ziegler‐Nichols tuning rules for PI control. Asian Journal of Control, 4(4): 364-380. https://doi.org/10.1111/j.1934-6093.2002.tb00076.x

[8] Tan, W., Liu, J., Chen, T., Marquez, H.J. (2006). Comparison of some well-known PID tuning formulas. Computers & Chemical Engineering, 30(9): 1416-1423. https://doi.org/10.1016/j.compchemeng.2006.04.001

[9] Visioli, A. (2012). Research trends for PID controllers. Acta Polytechnica, 52(5). https://doi.org/10.14311/1656

[10] Valério, D., Da Costa, J.S. (2006). Tuning of fractional PID controllers with Ziegler–Nichols-type rules. Signal Processing, 86(10): 2771-2784. https://doi.org/10.1016/j.sigpro.2006.02.020

[11] Maghade, D.K., Patre, B.M. (2014). Pole placement by PID controllers to achieve time domain specifications for TITO systems. Transactions of the Institute of Measurement and Control, 36(4): 506-522. https://doi.org/10.1177/0142331213508803

[12] Bingul, Z., Karahan, O. (2018). Comparison of PID and FOPID controllers tuned by PSO and ABC algorithms for unstable and integrating systems with time delay. Optimal Control Applications and Methods, 39(4): 1431-1450. https://doi.org/10.1002/oca.2419

[13] Goldberg, D.E. (2002). Genetic algorithms in search, optimization, and machine learning. 5th edition Pearson Education.

[14] Kennedy, J., Eberhart, R. (1995). Particle swarm optimization. In Proceedings of ICNN'95-international conference on neural networks, Perth, WA, Australia, pp. 1942-1948. https://doi.org/10.1109/ICNN.1995.488968

[15] Martínez-Soto, R., Castillo, O., Aguilar, L.T. (2014). Type-1 and Type-2 fuzzy logic controller design using a Hybrid PSO–GA optimization method. Information Sciences, 285: 35-49. https://doi.org/10.1016/j.ins.2014.07.012

[16] Şen, M.A., Bakırcıoğlu, V., Kalyoncu, M. (2016). Performances comparison of the bees algorithm and genetic algorithm for PID controller tuning. In Proceedings of the 5th International Conference on Mechatronics and Control Engineering, pp. 126-130. https://doi.org/10.1145/3036932.3036951

[17] Pham, D.T., Castellani, M. (2014). Benchmarking and comparison of nature-inspired population-based continuous optimisation algorithms. Soft Computing, 18(5): 871-903. https://doi.org/10.1007/s00500-013-1104-9

[18] Sharma, P., Gupta, R. (2014). Tuning of PID controller for a linear BLDC motor using TLBO technique. In 2014 International Conference on Computational Intelligence and Communication Networks, Bhopal, India, pp. 1224-1228. https://doi.org/10.1109/CICN.2014.254

[19] Yousri, D., Abd Elaziz, M., Mirjalili, S. (2020). Fractional-order calculus-based flower pollination algorithm with local search for global optimization and image segmentation. Knowledge-Based Systems, 197: 105889. https://doi.org/10.1016/j.knosys.2020.105889

[20] Pham, Q.V., Mirjalili, S., Kumar, N., Alazab, M., Hwang, W.J. (2020). Whale optimization algorithm with applications to resource allocation in wireless networks. IEEE Transactions on Vehicular Technology, 69(4): 4285-4297. https://doi.org/10.1109/TVT.2020.2973294

[21] Ghith, E.S., Tolba, F.A., Hammad, S.A. (2022). Real-time implementation of tuning PID controller based on sine cosine algorithm for micro-robotics system. In International Conference on Digital Technologies and Applications, pp. 801-811. https://doi.org/10.1007/978-3-031-02447-4_82

[22] Ghith, E.S., Tolba, F.A.A. (2022). Real-time implementation of tuning PID controller based on whale optimization algorithm for micro-robotics system. In 2022 14th International Conference on Computer and Automation Engineering (ICCAE), pp. 103-109. https://doi.org/10.1109/ICCAE55086.2022.9762448

[23] Ghith, E.S., Tolba, F.A.A. (2022). Design and

optimization of PID controller using various algorithms for micro-robotics system. Journal of Robotics and Control (JRC), 3(3): 244-256. https://doi.org/10.18196/jrc.v3i3.14827
[24] Ghith, E.S., Tolba, F.A.A. (2022). Real-time implementation of an enhanced PID controller based on marine predator algorithm (MPA) for micro-robotics system. In 2022 3rd International Conference on Artificial Intelligence, Robotics and Control (AIRC), pp. 40-45. https://doi.org/10.1109/AIRC56195.2022.9836454
[25] Ghith, E.S., Tolba, F.A.A. (2022). Real-time implementation of an enhanced proportional-integral-derivative controller based on sparrow search algorithm for micro-robotics system. IAES International Journal of Artificial Intelligence, 11(4): 1395-1404. http://doi.org/10.11591/ijai.v11.i4.pp%25p
[26] Ghith, E.S., Tolba, F.A.A. (2022). LabVIEW implementation of tuning PID controller using advanced control optimization techniques for micro-robotics system. International Journal of Mechanical Engineering and Robotics Research, 11(9): 653-661. http://doi.org/10.18178/ijmerr.11.9.653-661
[27] Bhuyan, M., Das, D.C., Barik, A.K. (2019). A comparative analysis of DSM-based autonomous hybrid microgrid using PSO and SCA. In 2019 IEEE Region 10 Symposium (TENSYMP), pp. 765-770. https://doi.org/10.3390/en14248276
[28] Misaghi, M., Yaghoobi, M. (2019). Improved invasive weed optimization algorithm (IWO) based on chaos theory for the optimal design of PID controller. Journal of Computational Design and Engineering, 6(3): 284-295. https://doi.org/10.1016/j.jcde.2019.01.001
[29] Singh, A., Suhag, S. (2020). Frequency regulation in an AC microgrid interconnected with a thermal system employing multiverse-optimized fractional order-PID controller. International Journal of Sustainable Energy, 39(3): 250-262. https://doi.org/10.1080/14786451.2019.1684286
[30] Li, S., Chen, H., Wang, M., Heidari, A.A., Mirjalili, S. (2020). Slime mould algorithm: A new method for stochastic optimization. Future Generation Computer Systems, 111: 300-323. https://doi.org/10.1016/j.future.2020.03.055
[31] Ahmed, Y., Hoballah, A., Hendawi, E., Al Otaibi, S., Elsayed, S.K., Elkalashy, N.I. (2021). Fractional order PID controller adaptation for PMSM drive using hybrid grey wolf optimization. International Journal of Power Electronics and Drive Systems (IJPEDS), 12(2): 745-756. https://doi.org/10.11591/ijpeds.v12.i2
[32] Acharya, B.B., Dhakal, S., Bhattarai, A., Bhattarai, N. (2021). PID speed control of DC motor using meta-heuristic algorithms. International Journal of Power Electronics and Drive Systems, 12(2): 822-831. https://doi.org/10.11591/ijpeds.v12.i2
[33] Abdulhussein, K.G., Yasin, N.M., Hasan, I.J. (2021). Comparison between butterfly optimization algorithm and particle swarm optimization for tuning cascade PID control system of PMDC motor. International Journal of Power Electronics and Drive Systems, 12(2): 736-744. https://doi.org/10.11591/ijpeds.v12.i2
[34] Ahmad, M.S., Ishak, D., Leong, T.T., Mohamed, M.R. (2021). Optimization of double stator PMSM with different slot number in inner and outer stators using genetic algorithm. International Journal of Power Electronics and Drive Systems, 12(2): 726-735. https://doi.org/10.11591/ijpeds.v12.i2
[35] Abbas, A.I., Anwer, A. (2022). The optimal solution for unit commitment problem using binary hybrid grey wolf optimizer. International Journal of Electrical & Computer Engineering, 12(1): 122-130. https://doi.org/10.11591/ijece.v12i1
[36] Ali, M.H.M., Mohamed, M.M.S., Ahmed, N.M., Zahran, M.B.A. (2022). Comparison between P&O and SSO techniques based MPPT algorithm for photovoltaic systems. International Journal of Electrical & Computer Engineering, 12(1): 32-40. https://doi.org/10.11591/ijece.v12i1
[37] Abdulhussein, K.G., Yasin, N.M., Hasan, I.J. (2022). Comparison of cascade P-PI controller tuning methods for PMDC motor based on intelligence techniques. International Journal of Electrical & Computer Engineering, 12(1): 1-11. https://doi.org/10.11591/ijece.v12i1
[38] Chinda, P.R., Rao, R.D. (2022). A binary particle swarm optimization approach for power system security enhancement. International Journal of Electrical & Computer Engineering, 12(2): 1929-1936. https://doi.org/10.11591/ijece.v12i2
[39] Alsmadi, M.K., Alzaqebah, M., Jawarneh, S., Brini, S., Al-Marashdeh, I., Briki, K., Al Refai, N.A., Alghamdi, F.A., Al-Rashdan, M.T., Khalil, M. (2022). Cuckoo algorithm with great deluge local-search for feature selection problems. International Journal of Electrical & Computer Engineering, 12(4): 4315-4326. http://dx.doi.org/10.11591/ijece.v12i4.pp4315-4326
[40] Reddy, A.C.O., Madhavi, K. (2022). Manta ray optimized deep contextualized bi-directional long short-term memory based adaptive galactic swarm optimization for complex question answering. International Journal of Electrical & Computer Engineering, 12(4): 3994-4006. http://doi.org/10.11591/ijece.v12i4.pp3994-4006
[41] Aribowo, W., Supari, B.S. (2022). Optimization of PID parameters for controlling DC motor based on the aquila optimizer algorithm. International Journal of Power Electronics and Drive Systems (IJPEDS), 13(1): 808-2814. https://doi.org/10.11591/ijpeds.v13.i1
[42] Astrom, K.J., Hagglund, T. (1995). PID Controllers: theory, design, and tuning. 2nd ed.: NC: Instrument Society of America.
[43] Eissa, M.M., Virk, G.S., AbdelGhany, A.M., Ghith, E.S. (2013). Optimum induction motor speed control technique using genetic algorithm. Am. J. Intell. Syst, 3(1): 1-12. https://doi.org/10.5923/j.ajis.20130301.01
[44] Eissa, M.M., Virk, G.S., AbdelGhany, A.M., Ghith, E.S. (2013). Optimum induction motor speed control technique using particle swarm optimization. International Journal of Energy Engineering, 3(2): 65-73. https://doi.org/10.5923/j.ijee.20130302.04
[45] Sallam, M., Saif, I., Saeed, Z., Fanni, M. (2020). Lyapunov-based control of a teleoperation system in presence of time delay. In International Conference on Advanced Intelligent Systems and Informatics, pp. 759-768. https://doi.org/10.1007/978-3-030-58669-0_67
[46] Mirjalili, S., Mirjalili, S.M., Lewis, A. (2014). Grey wolf optimizer. Advances in Engineering Software, 69: 46-61. http://dx.doi.org/10.1016/j.advengsoft.2013.12.007

[47] Manjarres, D., Landa-Torres, I., Gil-Lopez, S., Del Ser, J., Bilbao, M.N., Salcedo-Sanz, S., Geem, Z.W. (2013). A survey on applications of the harmony search algorithm. Engineering Applications of Artificial Intelligence, 26(8): 1818-1831. https://doi.org/10.1016/j.engappai.2013.05.008

[48] Pradhan, R., Majhi, S.K., Pati, B.B. (2018). Design of PID controller for automatic voltage regulator system using Ant Lion Optimizer. World Journal of Engineering.

NOMENCLATURE

PID	Proportional-integral-derivative
GWO	Grey Wolf Optimization
HS	Harmony Search algorithm
ALO	Ant Lion Optimization
IAE	Integral Absolute Error
ISE	Integral Square Error
ITAE	Integral of Time multiplied Absolute Error
ITSE	Integral of Time multiplied square Error
ISTES	Integral Square Time multiplied square
ISTSE	Integral of Square Time multiplied by square Error.
MIS	Minimal Invasive Surgery

Greek symbols

K_p	Proportional gain
K_i	Integral gain
K_d	Derivative gain
R	Radius
ρ	Density of Water
ζ	Dynamic Viscosity
m	Mass
cd	Drag Coefficient